NJC

Accepted Manuscript

This is an *Accepted Manuscript*, which has been through the Royal Society of Chemistry peer review process and has been accepted for publication.

Accepted Manuscripts are published online shortly after acceptance, before technical editing, formatting and proof reading. Using this free service, authors can make their results available to the community, in citable form, before we publish the edited article. We will replace this *Accepted Manuscript* with the edited and formatted *Advance Article* as soon as it is available.

You can find more information about *Accepted Manuscripts* in the Information for Authors.

Please note that technical editing may introduce minor changes to the text and/or graphics, which may alter content. The journal's standard Terms & Conditions and the Ethical guidelines still apply. In no event shall the Royal Society of Chemistry be held responsible for any errors or omissions in this *Accepted Manuscript* or any consequences arising from the use of any information it contains.

ROYAL SOCIETY OF CHEMISTRY

www.rsc.org/njc

Table of Contents Entry

Room temperature gas sensing properties of tubular hydroxyapatite

Li Huixia, Liu Yong *,Tan Yanni*, Luo Lanlan, Zhang Qing, Li Kun, Tang hanchun

Tubular hydroxyapatite was synthesized and showed high response, selectivity, good reproducibility and short response and recovery time to ammonia.

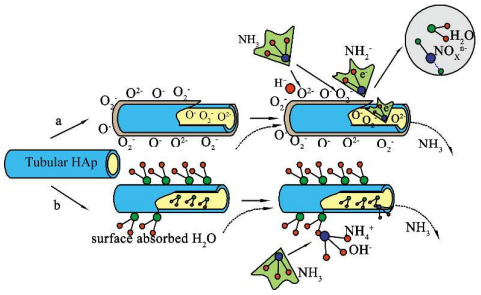

Room temperature gas sensing properties of tubular hydroxyapatite

Li Huixia, Liu Yong *, Tan Yanni*, Luo Lanlan, Zhang Qing, Li Kun, Tang hanchun

State Key Laboratory of Powder Metallurgy, Central South University, Changsha 410083, PR China

*Corresponding Author, Liu Yong,e-mail: yonliu@csu.edu.cn;

Tan Yanni, e-mail: tanyanni@csu.edu.cn

Abstract:

Tubular hydroxyapatite (HAp) was prepared by a combined method of cation exchange membrane-assisted and electrochemical deposition. For comparison, rod-like HAp was also fabricated by the hydrothermal method. The products were characterized by scanning electron microcopy (SEM), X-ray diffraction analysis (XRD) and Brunauer-Emmett-Teller (BET). The gas sensing properties to ammonia were studied particularly. The selectivity to various volatile organic compounds was also investigated, then, the response and the recovery time were determined. Results showed that the hollow mesoporous and nanocrystalline nature is the key factor that increases the sensing properties of HAp. Tubular HAp based sensors exhibit 1.35-1.65 times of response value to ammonia than the rod-like based one. At the concentration of ammonia of 2000ppm, the response value of HAp tubes was up to 84.58%, and the response time was as short as 10 s. Even at a low concentration of 50ppm, the response was still detectable. Furthermore, tubular HAp shows great stability and reproducibility for gas sensing. Results also indicated that tubular HAp has obvious

response to various gases, but has the highest response to ammonia. The growth mechanism of tubular HAp and the gas sensing mechanisms were proposed.

Keywords: tubular; hydroxyapatite; gas sensor; ammonia; volatile organic compounds; growth mechanism; sensing mechanism

1. Introduction

The detection of toxic gases such as NH_3 and various VOCs has become an important issue due to the increasing concern about environmental protections, emission control and human health[1]. Compared to commonly used optical methods, calorimetric methods, gas chromatograph and acoustic methods, the chemiresistive gas sensor exhibits the advantages of low energy consumption, non-destruction, cost effectiveness, high sensitivity and low detection limit, which makes them more appropriate for the application in the daily life[2, 3]. Nowadays, semiconducting oxides like SnO_2[4], ZnO[5], TiO_2[6], CuO[7] have been studied to detect flammable gases such as H_2, CO and CH_4. However, those sensors lack of specificity and sensitivity to toxic gases at low concentrations. Furthermore, the operation temperature usually is as high as 300 ℃ or above. Organic semiconductors[8, 9] (polypyrrole, polyanilineand, phthalocyanine) also draw much attention to detect alcohols, ammonia, chlorinated hydrocarbons, and nitrogen oxide gases. Nevertheless, due to their highly ordered and porous structures, the response and the recovery time often last several minutes even hours. Therefore, hydroxyapatite as one kind of extensively used biological inorganic material attracted lots of researchers' attention from different fields[10-13].

Hydroxyapatite [HAp,$Ca_{10}(PO_4)_6(OH)_2$] has been extensively used in biomedical applications due to its excellent biocompatibility and bioactivity[14, 15]. In addition, it also has other applications such as chromatography[16], biosensors[17], catalyst[18] and fuel cell[19]. Recently, because of the unique properties like high porosity and strong capability to exchange ions, HAp has been paid considerable attentions as a chemical gas sensor. Mene et al[1, 20]have studied the gas sensing properties of HAp films for CO and CO_2, but found that the resistance of HAp film is very high, and the sensitivity is quite low even for high gas concentration at room temperature. Furthermore, the best sensitivity at 165℃ for 1000ppm is only about 35%. Some methods have been tried to improve the gas sensing property of HAp by means of swift heavy ion irradiation[21, 22] or doping of Si, Fe or Co[10, 23]. Unfortunately, the enhancement is relatively limited. HAp used in the previous study for gas sensing was usually made from chemical precipitation method with non-uniform agglomerate structures. Actually, the gas sensing properties of ceramic or polymers are highly dependent on their surface morphology. Therefore, it is possible to increase the gas sensing properties of HAp by adjusting its morphology. HAp with complicated three-dimensional(3D) morphology such as flower-like, dandelion-like, bowknot-like and sea cucumber-like agglomeration have been prepared by hydrothermal method[24, 25], rapid microwave method[26], electrochemical deposition method[27] and template-assisted method[28] with the help of chelating agent, surfactant or template, respectively. The effects of the morphology on the gas sensing properties of HAp have not been studied, and the

application of HAp to detect volatile organic compounds (VOCs) and toxic gases has been rarely reported.

In the present work, HAp powders with rod-like and tubular structure were prepared. The morphology, phase constitution, specific surface area and the pore distribution were characterized, and six different kinds of toxic VOCs and ammonia were used for gas sensing measurement. The gas sensing properties of HAp with different morphology were compared.

2. Materials and methods

2.1 Material preparation

Nafion N-117 cation-exchange membrane, $Ca(NO_3)_2 \cdot 4H_2O$ and $(NH_4)_2HPO_4$were purchased from Alfa Aesar. All other chemicals were of analytical reagent grade. Deionized water (DI water, ULUP-1-20T) was used as solvent in all experiments. Rod-like HAp was prepared by the hydrothermal method. Firstly, the pH value of $(NH_4)_2HPO_4$ solution was adjusted to 9 by adding ammonium hydroxide (30%). $(NH_4)_2HPO_4$ (20mlof 0.3M) solution was added dropwise into $Ca(NO_3)_2 \cdot 4H_2O$ (20ml of 0.5M), which was vigorously stirred. Then, the mixed solution was transferred into a Teflon lined stainless steel autoclave (100ml), and placed in an air blowing dry oven at 150℃ for 24h. Finally, the autoclave was cooled to room temperature, and the solution was filtered. The precipitate was washed with distilled water and dried at 60 ℃ for 12h. Tubular HAp was prepared by a combination of cation exchange membrane-assisted electrochemical deposition method. 0.5M $Ca(NO_3)_2 \cdot 4H_2O$ and

0.3M$(NH_4)_2HPO_4$（the pH value was adjusted to 11 in advance）solutions were added into two cylindrical glass containers, respectively. A cation-exchange membrane was fixed in the middle of the containers. On each side, there was a platinum electrode, and the electrochemical deposition was conducted at 3 V and 50℃ for 1h. Then, the whole device was put into an air blowing oven at 50℃, and held for 7 days. Finally, the membrane was taken out, rinsed gently, dried at 60 ℃, and the powder on the membrane was collected.

2.2 Material characterization

Powder X-ray diffraction(XRD; Rigaku D/max 2500PC, Japan)was carried out using CuK_α radiation (λ=1.54178Å) at 40 kV in steps of 0.02° from diffraction angles (2θ) 5 to 80°. Crystallinity was calculated from the XRD results using the JADE analysis software. The morphology of HAp agglomerates were characterized by field emission scanning electron microscopy (FESEM, JEOL JSM-6700F, Japan). Nitrogen adsorption-desorption isotherms were obtained using Autosorb-1 (Quantachrome Instruments). The specific surface area was measured by the Brunauer-Emmett-Teller (BET) method using adsorption isotherms. The distribution of the pore size was calculated by the Barrett-Joyner-Halenda method using desorption isotherms.

2.3 Measurements of gas sensing properties

(a) Preparation of gas sensors: about 1.25 mg HAp was mixed with several drops of pure water to form a paste, and then coated onto the outside surface of a ceramic tube for each sensor. The thickness on the sensor was about 200μm in average. At

least 5 sensors were prepared for each measurement. There are a pair of gold electrodes at each end of the ceramic tube. Each electrode of the ceramic tube was connected with two Pt wires and a Ni–Cr heating filament. Finally, the total six tentacles were welded on a hexangular base to form a gas sensor. The structure and schematic diagram of the sensor are shown in Fig. 1 (a, b).

(b) Measurement of gas sensing properties: gas sensing properties were measured by a CGS-8 (Chemical gas sensor-8) intelligent gas sensing analysis system (Beijing Elite Tech Co.,Ltd., China) at room temperature (25℃).The measuring schematics are shown in Fig.1(c). The resistance of the sensor in clean air and target gas can be measured by this way. In the process of testing the gas sensing properties, saturated target gas was injected into an evaporator in the plastic test chamber (20 dm^3 in volume) (Fig. 1(a)), and there is a fan to help diffuse and mix homogeneously with the air. The volume of target gas injected is calculated by the following formula:

$$Q=(V\times C\times M)/(22.4\times d\times \rho)\times 10\text{-}9\times(273+T_R)/(273+T_B) \quad (1)$$

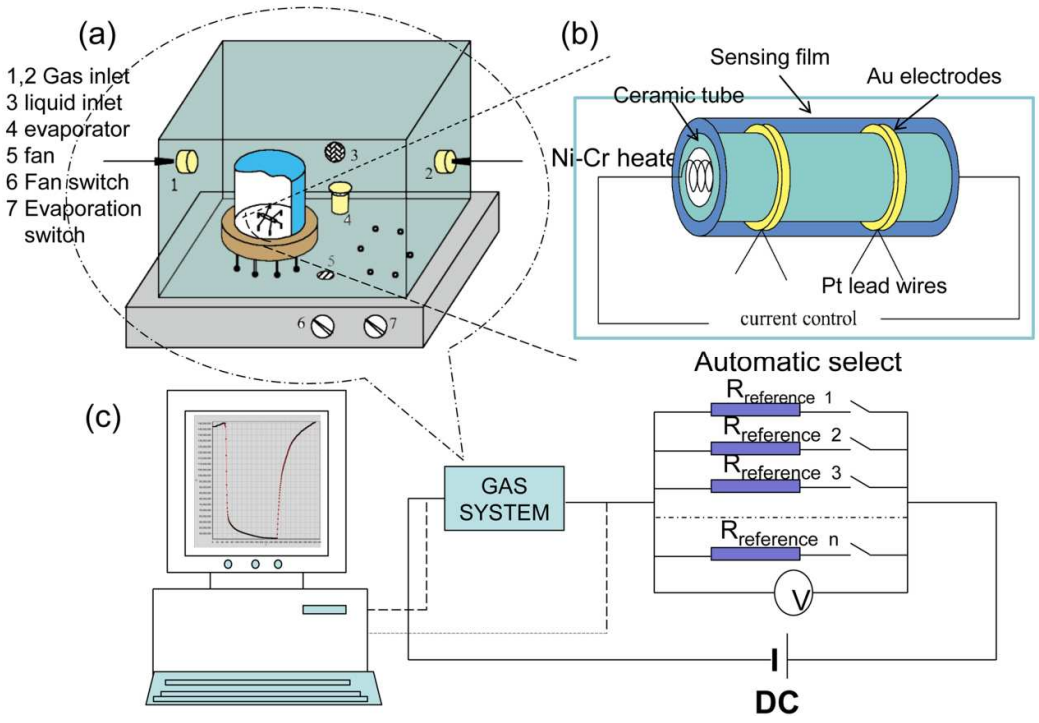

Fig. 1 Gas sensing device (a), ceramic tube (b) and measuring schematics of the CGS-8 intelligent gas sensing analysis system (c).

Q is the volume of target gas; V is the volume of the test chamber; C is the target gas concentration we need (ppm); M is the molecular weight (g); d is the density of target gas (g/cm^3); ρ is the purity of target gas; T_R is the temperature of the test environment (℃); T_B is the temperature in the test chamber (℃). Target gases include ammonia (NH_3) and VOCs such as acetone (C_3H_6O), toluene (C_7H_8), n-hexane (C_6H_{14}), n-heptane (C_7H_{16}), n-decane ($C_{10}H_{22}$) and styrene (C_8H_8). The target gases with high purity (above 99.5%) were commercial available. The response of the sensor was calculated by the equation: S=(Ra-Rg)/Ra, where S is the response value, Ra and Rg represent the sensor's resistance in air and target air respectively. The response time and the recovery time were defined as the time

taken by the sensor to achieve 90% of the total resistance change in the cases of response (target gas adsorption) and recovery (target gas desorption), respectively.

3. Results

Hydroxyapatite with rod-like and tubular morphologies were successfully prepared by the hydrothermal method and a combined method of cation exchange membrane-assisted and electrochemical deposition, respectively. The results about the morphologies, phase constitution, specific surface area and gas sensing properties of the synthesized hydroxyapatite were described in the following sections.

3.1 Morphology of HAp

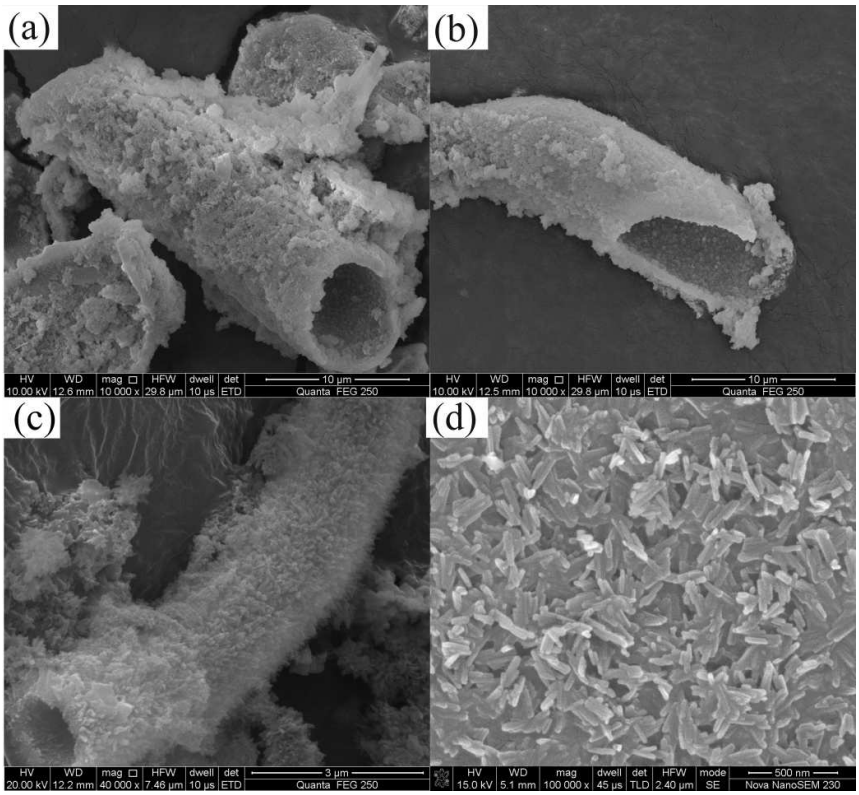

Fig. 2 SEM image of HAp prepared by membrane assisted electrochemical deposition method (a, b, c) and hydrothermal method (d).

Fig.2 shows the morphology of HAp prepared by two methods. It can be seen clearly that most of the HAp prepared from electrochemical deposition method has a tubular structure with a diameter of 2.5-5μm, and a length of 5-20μm (Fig. 2(a, b, c)). Fig. 2(c) also shows the surface of the tubular HAp consists of clusters of nanorods. The scattered particles are clusters, which may fall out from the tube during the preparation of the SEM samples. HAp prepared by the hydrothermal method is well dispersed and rod-like with a diameter of 15-30nm, and a length of 100-300nm (Fig. 2(d)).

3.2 Phase constitution

The composition and the phase structure of HAp are shown in Fig. 3. It is clear that the diffraction patterns of the products are consistent with the standard pattern of HAp (PDF 09-0432), with no evidence of secondary crystal phase. It is obviously that rod-like HAp has a higher crystallinity (97.5%) than the tubular HAp (86.87%). Moreover, the (002) diffractions of both HAp are very sharp and intense, which indicates some preferred crystal orientation of (002), i.e. c-axis.

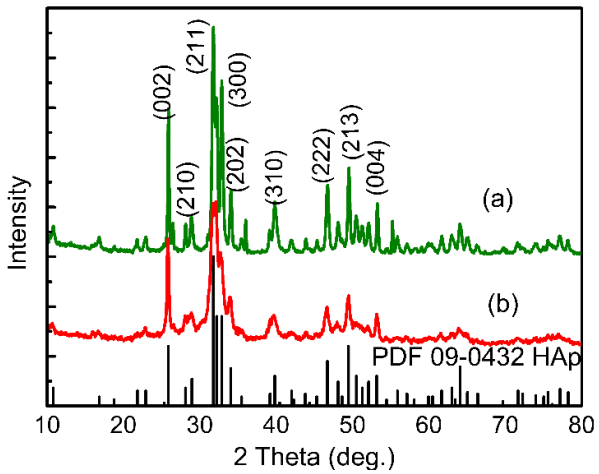

Fig. 3 XRD patterns of rod-like HAp (a) and tubular HAp (b).

3.3 Specific Surface Area (SSA)

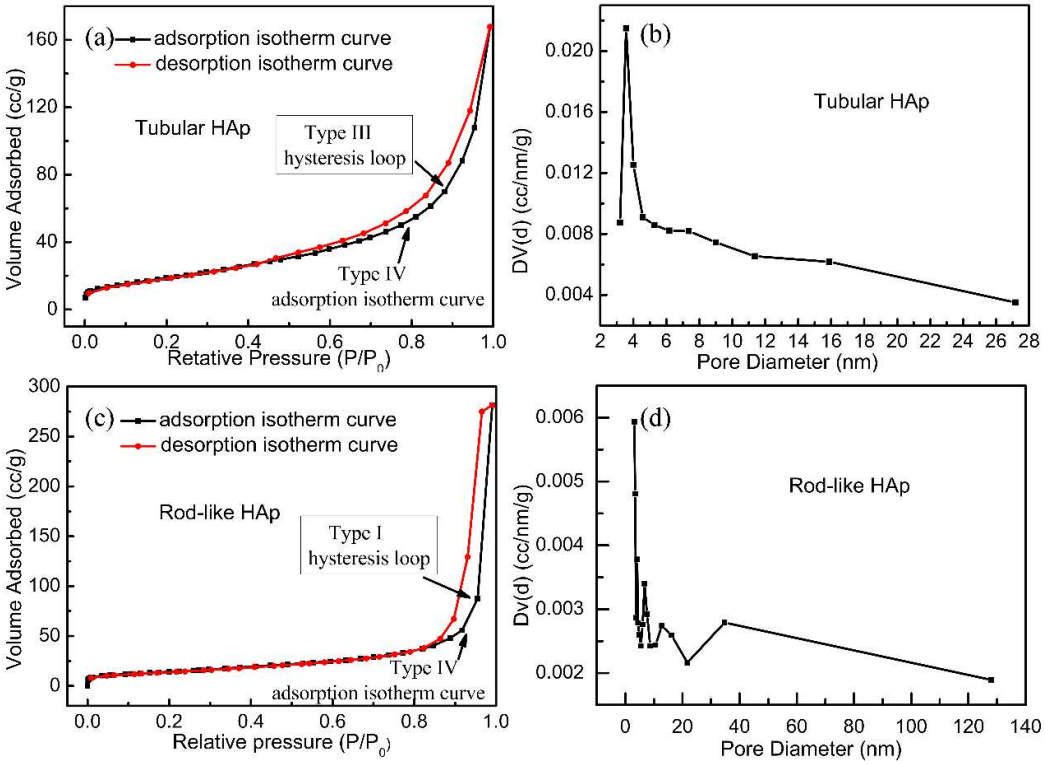

Fig. 4 Adsorption isothermal curves (a) & (c) and pore distributions (b)&(d) of tubular HAp (a)&(b) and rod-like HAp(c)&(d).

Fig. 4 shows the N_2 adsorption/desorption isotherm and the corresponding pore size distribution of HAp with different morphology. The distinct adsorption isotherm curve for the samples can be categorized as type Ⅳ which suggests a physical adsorption with capillary condensation phenomenon. Furthermore, the adsorption isotherm of tubular HAp exhibits a hysteresis loop of type Ⅲ[29] (Fig. 4(a)). The pore distribution analysis shows a mesoporous nature, and the pore size is mostly in 3-30nm (Fig. 4(b)). The measurement shows a SSA of 74.245 m^2/g, an average pore diameter of 14.62nm and a total pore volume of 0.2596 cc/g for tubular HAp. However, for rod-like HAp

(Fig. 4(c, d)), the SSA is only 40.295 m^2/g with an average pore diameter of 33.71nm. The hysteresis loop of type Ⅰ indicates a uniform dimension of rod-like HAp agglomerates.

3.4 Gas sensing properties

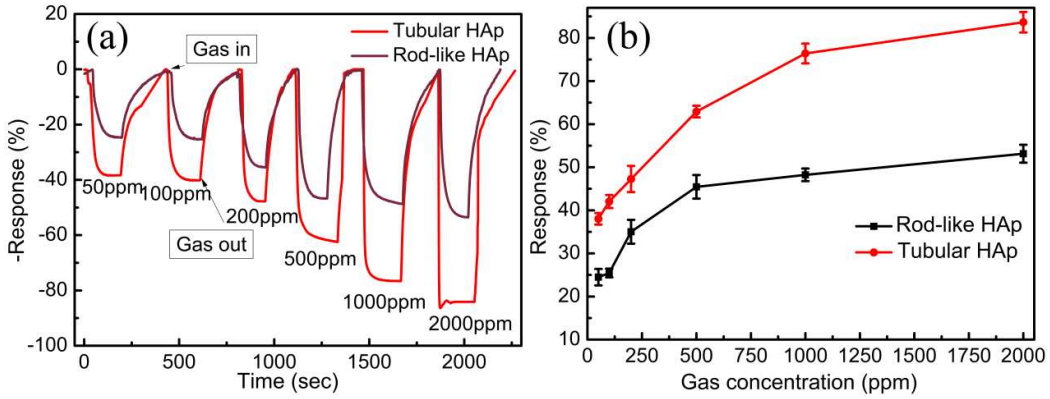

Fig. 5 Response vs time curves (a) and response vs ammonia concentration (b) at room temperature for rod-like and tubular hydroxyapatite in the range of 50-2000ppm.

The gas sensing properties of two kinds of HAp were studied at room temperature. Fig.5(a) shows the response and recovery curves of rod-like HAp and tubular HAp to different concentrations of NH_3 ("-" of the ordinate stands for the decrease of the resistance when HAp sensor is exposed to reducing gases.). It can be seen clearly that when the sensor is exposed into ammonia gas, the resistance decreases rapidly and reaches a minimum value. When the sensor is taken out, the gas absorbed is released and the resistance recovers to the initial value. Tubular HAp based sensor shows a much larger response magnitude to each ammonia concentration compared with rod-like HAp based sensor. Furthermore, tubular HAp sensor responses more quickly than rod-like HAp ones, with response time of 50, 45, 35, 30, 18, 10 sec for tubular HAp sensor and 56, 62, 66, 45, 57, 55 sec for rod-like HAp sensor at gas

concentrations of 50, 100, 200, 500, 1000, 2000 ppm, respectively. Most of the recovery time of tubular HAp (94, 121, 107, 138, 128, 180 sec) is shorter than that of rod-like HAp (178, 149, 120, 86, 147, 124 sec at gas concentrations of 50, 100, 200, 500, 1000, 2000 ppm, respectively). The possible reason is that the structure of rod-like HAp is simple, while the structure of tubular HAp is complicated. The unique properties of tubular HAp including tube morphology, high specific surface area and mesoporous feature, make it has more adsorption sites for gas molecules. So the tubular HAp sensors respond and recover more quickly than rod-like HAp sensors. From Fig. 5(b), it can be seen that, at concentration from 50 ppm to 1000 ppm for tubular HAp (from 50 ppm to 500 ppm for rod-like HAp), the response increases almost linearly due to the unimolecular layer of gas molecules formed on the surface of the sensor. Then, at high gas concentrations, the multilayers of gas molecules on the sensor surface result in the saturation. The response sensitivity of tubular HAp is 1.35-1.65 times higher than that of rod-like HAp. The response sensitivity of tubular HAp to NH_3 at 2000ppm reaches 84.58%. So, in the following study, more attention was paid on the gas sensing properties of tubular HAp.

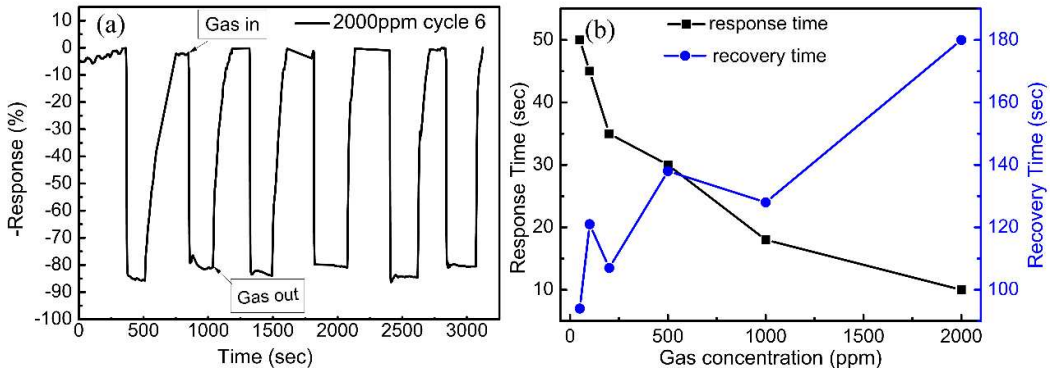

Fig. 6 Continues cycles of 2000ppm ammonia gas (a) and response/ recover time vs. gas concentration (b) for tubular hydroxyapatite.

To investigate the stability and the reproducibility of tubular HAp based sensor, 6 cycles to NH_3 at 2000ppm were repeated. It indicates a good reproducibility with a relatively small deviation (Fig. 6(a)). Moreover, the response and the recovery time to different concentrations of NH_3 were compared. Generally, with the increase of the concentration of NH_3 from 50 ppm to 2000 ppm, the response time decreases from 50s to 10s while the recovery time increases from 94s to 180s (Fig. 6(b)). This trend was also reported in previous literatures[30-32]. With the increasing of ammonia concentration, the number of ammonia molecules to interact with the sensing surface becomes higher, and the desorption of higher concentration of ammonia is prolonged. To assess the response and recovery time of tubular HAp, the sensing properties of other materials to ammonia were summarized from literatures reported in latest years, as shown in Table 1. Compared with other materials, it can be seen clearly that the tubular shows shorter response and recovery time even at room temperature.

Table. 1 NH_3 sensing property of tubular HAp compared with other gas sensor reported in several recently literatures.

Sensing materials	Ammonia Concentration	Working temperature	Response/ Recovery time	References
Pt/AlGaN/GaN	10ppb	115℃	19.43min/36.67min	Sensors&Actuator B: chemical,2014[33]
	1000ppm		8.73min/2.04min	
CeO_2	500ppm	RT	64min/51min	Current Applied Physics,2014[34]

graphene–PEDO:PSS	500ppm	RT	~3min/5min	Organic Electronics,2014[35]
$LaFeO_3$	50ppm	550℃	~1000s/1500s	Ieee Sensors Journal,2015[36]
Co_3O_4/SiO_2	60ppm	RT	~50s/125	Journal of Hazardous Materials,2014[37]
Graphene/mica	50ppm	RT	~1min/1min	Applied Physics Letters,2014[38]
silver nanowires	500ppm	RT	70min/100min	Sensors&Actuators A: Physical,2014[39]
Carbon nanoflake/tin oxide composites	100ppm	350℃	200s/5min	Journal of Hazardous Materials,2014[40]
Tubular HAp	50ppm 2000ppm	RT	50s/94s 10s/180s	This work

RT: room temperature

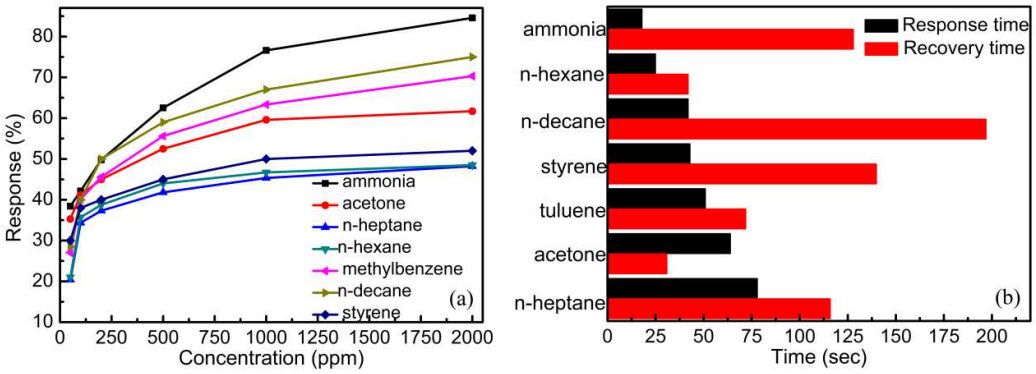

Fig. 7 Responses of tubular hydroxyapatite vs. concentrations of different gases (a) and response/recover time comparison of different gases at 1000 ppm (b).

To test the selectivity of tubular HAp to different gases, six kinds of gases including acetone, toluene, n-hexane, n-heptane, n-decane and styrene were chosen for study. As shown in Fig.7 (a), tubular HAp sensor has obvious response to various volatile organic gases, and the response sensitivity at 2000ppmis: ammonia (84.58%)> n-decane (75.2%) > toluene (73.3%) > acetone (61.7%) > styrene (52.0%) > n-hexane (48.5%) > n-heptane (48.22%). Therefore, tubular HAp exhibits the highest response to ammonia gas. To explain the different response and recovery time of tubular HAp

to various gases, the typical and representative set of data at 1000ppm was shown in Fig.7 (b), and the same trend appears at other concentrations. The response time to ammonia is the shortest(18 seconds), and that to n-heptane is the longest. However, for acetone, the recovery time is as short as 31 seconds and for n-decane the recovery time is nearly 200 seconds. The distinctions may be a result of differences in structures, functional groups, kinetic diameter[41], number of carbon atoms or the polarity of the gases[42, 43].Gases with special functional groups exhibit higher response(-NH_2>-C_6H_5>-C=O-), and the response/recovery time is relatively shorter. Styrene shows low response and long response/recovery time, possibly due to its oily liquid feature. For alkanes, the response increases with the increase of the number of carbon atoms, and the response/recovery time has the same trend.

4. Discussion

4.1 Formation mechanism of tubular HAp

Based on the above results, possible synthesis mechanism was proposed for the formation of tubular HAp. Ca^{2+} penetrated through from the parallel cylindrical water channels (polymer backbone on the outside and sulfonic ionic groups on the inside) of the Nafion N-117 membrane[44], and reacted with PO_4^{3-} and OH^- of the P-side to form HAp as below:

$$5Ca^{2+} + 3PO_4^{3-} + OH^- \rightarrow Ca_5\left(PO_4\right)_3 OH \qquad (2)$$

About the growing site of the tube, there are two hypotheses: “grown at the top of the tube” and “grown at the bottom of the tube”[45-47]. But the latter one was mostly approved, i.e. Ca^{2+} reacted with PO_4^{3-} and OH^- at the interface of the membrane and

the bottom of the tube[45], besides, Masakazu Takiguchi et.al[47] also proved this point by using a digital microscope in the process of producing calcium carbonate through the similar membrane-assisted method.

The possible formation mechanism of tube HAp (Fig. 8) is based on the results that only the spots containing ion-exchange sulfonic groups allow Ca^{2+} penetrate through the membrane. While the domains of defect and hydrophobic polymer backbone would stop $Ca^{2+}$from getting through so that HAp crystals would nucleate and grow avoiding those domains (a). Then, most of the membrane is covered with HAp crystals except the domains where calcium ions cannot pass. HAp crystals grow preferentially along c-axis to form lengthy nanosheets. Then, to reduce their surface energy, the nanosheets aggregate in a certain orientation to form follower-like clusters (b). As the clusters stack thicker, permeation of calcium ions becomes difficult so the calcium ions constantly transferred to the edge of those domains, then the edge of those domains would serve as a spring of calcium ions making the formation and growth of tubular HAp from the bottom[46, 47](c).

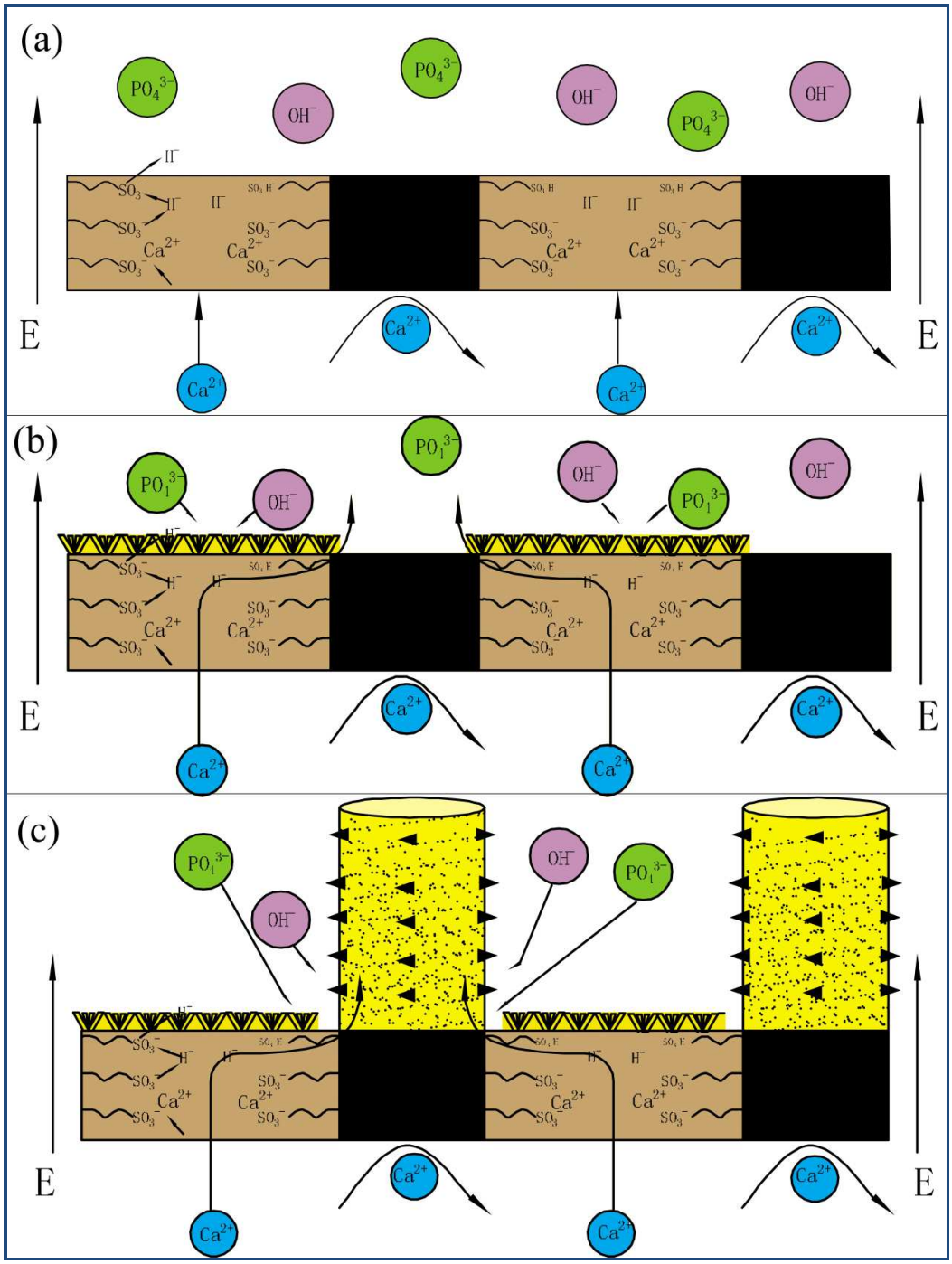

Fig. 8 Schematic illustration of major steps involved in the process of synthesizing tubular hydroxyapatite.

4.2 Gas sensing mechanism of tubular HAp

It is known that the porous HAp surface is enriched with several ionic species like Ca^{2+}, PO_4^{3-} and OH^-. The gas sensing properties depend on the resistance change induced by the adsorption and the desorption processes. The P-OH group on HAp surface can acts as an adsorption site for the target gases to be sensed. To understand the gas sensing properties, it is necessary to interpret the conductivity mechanism of HAp. Protons are acknowledged as the charge carriers in HAp crystals at room temperature, rather than calcium cations and phosphate ions. Protons migrate from OH^- to the adjacent PO_4^{3-} along c-axis channels[48-50]. From the XRD results, it can be found that HAp grows preferentially along (002) orientation, i.e c-axis, Due to the preferred growth orientation along (002),the amounts of OH channels and Ca channels out of wider c-planes were larger, which is probably beneficial for the adsorption of gas and the improvement of conductivity. Besides, tubular HAp exhibit poorer crystallinity than rod-like HAp, the huge specific surface energy and the high activity due to the high level of structural defects on HAp surface, which may be another reason for the superior gas sensing properties of tubular HAp. Furthermore, HAp with specific tubular structure, high surface-to-volume ratio and the mesoporous feature allow the target gas molecules to diffuse rapidly throughout the hollow tubes and sensing sites, resulting in a high response value and fast response speed. Finally, the gas sensing properties of tubular HAp may be due to the reaction between the physically absorbed target gases and the surface of HAp. The possible reaction mechanisms for gas sensing properties of HAp to ammonia and other volatile organic compounds are explained as follows.

306 .

307 The preferred orientation, poor crystallinity, special tubular morphology, large
308 specific surface area, and mesoporous structure of the tubular HAp provide more
309 adsorption sites for the adsorption of atmospheric oxygen on the sensor surfaces and
310 grain-boundaries, and then the oxygen extracts electrons from the conduction band to
311 become O_2^-, $O^-$and O^{2-}.

312 $$O_2\,(\text{gas}) \leftrightarrow O_2\,(\text{ads}) \quad (3)$$

313 $$O_2\,(\,(\text{ads})) + ne^- \leftrightarrow m\left(O_2^- / O^- / O^{2-}\right) \quad (4)$$

314 In addition, Laghzizil et al[51, 52]also proposed the reaction between the adjacent OH^-
315 and PO_4^{3-} in HAp.

316 $$OH^- + OH^- \leftrightarrow O^{2-} + HOH \quad (5)$$

317 $$OH^- + PO_4^{3-} \leftrightarrow O^{2-} + HPO_4^{2-} + OH \leftrightarrow O^{2-} + PO_4^{3-}HOH + \text{vacancy}OH^- \quad (6)$$

318 When the sensors are exposed to ammonia atmosphere, they capture NH_3 molecules
319 to the surface. NH_3 acts as a proton donor, and produces intermediates of NH^{2-} which
320 will react with O_2^-, O^- and O^{2-}. HAp crystals act as the proton acceptor, and the
321 resistance decreases due to the increment of the charge carrier. Besides, NO_x^{n-} can be
322 incorporated in the lattice of HAp crystals. It is more likely that NO_x^{n-}will replace
323 OH^- on the surface or in the channel of HAp crystal, then introduce slight change of
324 the framework of HA and induce a change of conductivity (Fig. 9(a)).

325 $$NH_3 \leftrightarrow NH_2^- + H^+ \quad (7)$$

$$NH_2^- + (O_2^- / O^{2-} / O^-) \leftrightarrow NO_x^{n-} + H_2O \quad (8)$$

Another possible mechanism of the high sensitivity of HAp to ammonia gas is supposed as follows: HAp is highly hydrophilic and the P-OH groups enriched on the surface can absorb H_2O from the environment at room temperature. When the HAp sensor is exposed to ammonia, the reaction between ammonia with physically adsorbed H_2O may happen on the surface of sensor. The proton conductivity via NH_4^+cations[53] increases, and the resistance will decrease remarkably since protons are acknowledged to be the charge carriers of HAp (Fig. 9(b).

$$NH_{3(g)} + H_2O_{(surface)} \overset{RT}{\leftrightarrow} NH_4^+{}_{(ads)} + OH^-_{(ads)} \quad (9)$$

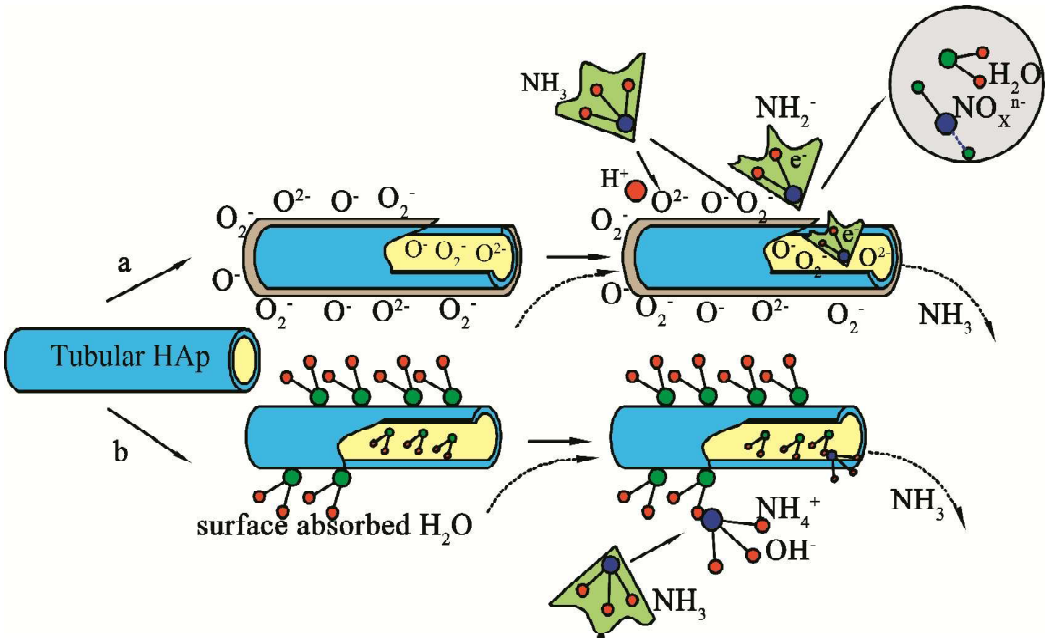

Fig. 9 Schematic illustration of major ammonia sensing mechanisms of tubular hydroxyapatite

When the sensor is exposed to other volatile organic compounds ($C_xH_yO_z$), the gas molecules will be absorbed and dissociate on the surface of the sensor, and the target

gas will act as a proton donator and increase the conductivity of HAp and produce intermediate compounds of $C_xH_{y-n}O_z^{n-}$. Then $C_xH_{y-n}O_z^{n-}$ will react with O_2^-, O^- and O^{2-} to produce CO_2 and H_2O or other products. Finally, the CO_2 may react with OH^- ions enriched on the surface of HAp to convert to CO_3^{2-}. The formation of CO_3^{2-} molecules is found to be also responsible for sensing behavior of HAp upon gas adsorption. Moreover, CO_3^{2-} may replace OH^- on the surface or in the channel of HAp crystal, and affect the crystal structure. Relevant processes are shown in the following equations:

$$C_xH_yO_z \leftrightarrow C_xH_{y-n}O^{n-} + nH^+ \quad (10)$$

$$C_x\,H_{y-n}O_z^{\,n-}{}_{(ads)} + m\left(O^{2-}/O^-/O_2^-\right)_{(ads)} \leftrightarrow CO_{2(g)} + H_2O_{(g)} + e^- \quad (11)$$

$$CO_2 + 2OH^- \leftrightarrow CO_3^{2-} + H_2O \quad (12)$$

5. Conclusions

Rod-like and tubular hydroxyapatite were prepared and characterized, and their gas sensing properties were studied. Compared to rod-like hydroxyapatite, tubular hydroxyapatite exhibits special three-dimensional structure, lower crystallinity, higher specific surface area and mesoporous feature, which provides more adsorption sites for the target gases to be sensed. So tubular hydroxyapatite sensors respond and recover more quickly than rod-like hydroxyapatite sensors. The sensing mechanisms of hydroxyapatite to various target gases depend on the reactions between the absorbed atmospheric oxygen (O^{2-}, O^-, O_2^-) and the intermediate compounds of gas molecules after donating protons. For ammonia, except for its smaller kinetic diameter and amino-group compared to various volatile organic compounds, the reaction between the physically absorbed H_2O and NH_3 increases the conductivity of protons via NH_4^+ cations, which may be another reason for the high sensitivity. In

general, tubular hydroxyapatite exhibits high sensitivity, quick response and recovery time, excellent reproducibility and selectivity. Thus, tubular hydroxyapatite is a promising material for gas sensors, and can be used in the trace detection of ammonia leakage in manufacturing industries of plastics, explosives, pesticides or chemical fertilizer, vehicle application and combustion.

Acknowledgment

This research was financially supported by the National Natural Science Foundation of China (No. 51272289).

References

[1] R. Mene, M. Mahabole, R. Aiyer,R. Khairnar, The Open Applied Physics Journal, 2010, 3, 10-16.

[2] X. Liu, S. Cheng, H. Liu, S. Hu, D. Zhang,H. Ning, Sensors, 2012, 12, 9635-9665.

[3] S. Sazhin, E. Soborover,S. Tokarev, Russian journal of nondestructive testing, 2003, 39, 791-806.

[4] L. V. Thong, L. T. N. Loan,N. Van Hieu, Sens. Actuators, B, 2010, 150, 112-119.

[5] J. Xu, Q. Pan, Y. a. Shun,Z. Tian, Sens. Actuators, B, 2000, 66, 277-279.

[6] H. G. Moon, Y. S. Shim, H. W. Jang, J. S. Kim, K. J. Choi, C. Y. Kang, J. W. Choi, H. H. Park,S. J. Yoon, Sens. Actuators, B, 2010, 149, 116-121.

[7] J. Tamaki, T. Maekawa, N. Miura,N. Yamazoe, Sens. Actuators, B, 1992, 9, 197-203.

[8] J. M. Slater, E. J. Watt, N. J. Freeman, I. P. May,D. J. Weir, Analyst, 1992, 117, 1265-1270.

[9] J. J. Miasik, A. Hooper,B. C. Tofield, Journal of the Chemical Society, Faraday Transactions 1: Physical Chemistry in Condensed Phases, 1986, 82, 1117-1126.

[10] R. U. Mene, M. P. Mahabole, K. Mohite,R. S. Khairnar, Mater. Res. Bull., 2014, 50, 227-234.

[11] P. Kanchana, N. Lavanya,C. Sekar, Materials Science and Engineering: C, 2014, 35, 85-91.

[12] E. Boanini, P. Torricelli, M. Gazzano, E. Della Bella, M. Fini,A. Bigi, Biomaterials, 2014, 35, 5619-5626.

[13] G. Bhardwaj,T. J. Webster, Northeast Bioengineering Conference (NEBEC), 2014 40th Annual, 2014, 1-2.

[14] P. Habibovic, F. Barrere, C. A. Blitterswijk, K. Groot,P. Layrolle, J. Am. Ceram. Soc., 2002, 85, 517-522.

[15] T.-M. G. Chu, D. G. Orton, S. J. Hollister, S. E. Feinberg,J. W. Halloran, Biomaterials, 2002, 23, 1283-1293.

[16] M. Urist, Y. Huo, A. Brownell, W. Hohl, J. Buyske, A. Lietze, P. Tempst, M. Hunkapiller,R. DeLange, Proc. Natl. Acad. Sci., 1984, 81, 371-375.

[17] B. Wang, J. J. Zhang, Z. Y. Pan, X. Q. Tao,H. S. Wang, Biosens. Bioelectron., 2009, 24, 1141-1145.

[18] V. J. Rasquinha, C. S. Ranawat,A. J. Mauriello Jr, J. Arthroplasty, 2002, 17, 113-117.

[19] K. Yamashita, H. Owada, T. Umegaki, T. Kanazawa,K. Katayama, Solid State Ionics, 1990, 40, 918-921.

[20] M. Mahabole, R. Aiyer, C. Ramakrishna, B. Sreedhar,R. Khairnar, Bull. Mater. Sci., 2005, 28, 535-545.

[21] R. U. Mene, M. P. Mahabole, R. Sharma,R. S. Khairnar, Vacuum, 2011, 86, 66-71.

[22] R. U. Mene, M. P. Mahabole,R. S. Khairnar, Radiat. Phys. Chem., 2011, 80, 682-687.

[23] M. P. Mahabole, R. U. Mene,R. S. Khairnar, Adv.Mater. Lett., 2013, 900, 1.

[24] A. Lak, M. Mazloumi, M. Mohajerani, A. Kajbafvala, S. Zanganeh, H. Arami,S. Sadrnezhaad, J. Am. Ceram. Soc., 2008, 91, 3292-3297.

[25] L. X. Yang, J. J. Yin, L. L. Wang, G. X. Xing, P. Yin,Q.-W. Liu, Ceram. Int., 2012, 38, 495-502.

[26] J. Liu, K. Li, H. Wang, M. Zhu,H. Yan, Chem. Phys. Lett., 2004, 396, 429-432.

[27] Q. Zhang, Y. Liu, Y. Zhang, X. Ji, Y. Tan,Q. Liu, Mater. Lett., 2013, 107, 337-339.

[28] Y. Zhang, Y. Liu, X. Ji, C. E. Banks,W. Zhang, Chem. Commun., 2011, 47, 4126-4128.

[29] D. H. E. K. S. W. Sing, R. A. W. Haul, Pure and applied chemisitry, 1985, 57, 603-619.

[30] S. Nalage, A. Mane, R. Pawar, C. Lee,V. Patil, Ionics, 2014, 20, 1607-1616.

[31] D. Dhawale, R. Salunkhe, U. Patil, K. Gurav, A. More,C. Lokhande, Sens. Actuators, B, 2008, 134, 988-992.

[32] G. K. Mani,J. B. B. Rayappan, Materials Science and Engineering: B, 2015, 191, 41-50.

[33] P.-C. Chou, H.-I. Chen, I.-P. Liu, C.-W. Hung, C.-C. Chen, J.-K. Liou,W.-C. Liu, Sens. Actuators, B, 2014, 203, 258-262.

[34] B. Renganathan, D. Sastikumar, A. C. Bose, R. Srinivasan,A. Ganesan, Current Applied Physics, 2014, 14, 467-471.

[35] Y. Seekaew, S. Lokavee, D. Phokharatkul, A. Wisitsoraat, T. Kerdcharoen,C. Wongchoosuk, Organic Electronics, 2014, 15, 2971-2981.

[36] T. Sathitwayakul, E. Newton, I. Parkin, M. Kuznetsov,R. Binions, 2015,

[37] Z.-J. L. Yong-Liang Tang, Jin-Yi Ma, Hai-Qiao Su, Yuan-Jun Guo, Lu Wang,,J.-J. C. Bo Du, Weilie Zhou, Qing-Kai Yu, Xiao-Tao Zu,, Journal of Hazardous Materials, 2014, 280, 127–133.

[38] Z. B. Aziza, Q. Zhang,D. Baillargeat, Applied Physics Letters, 2014, 105, 254102.

[39] L. Shobin, D. Sastikumar,S. Manivannan, Sensors and Actuators A: Physical, 2014, 214, 74-80.

[40] S.-K. Lee, D. Chang,S. W. Kim, Journal of hazardous materials, 2014, 268, 110-114.

[41] K. Suri, S. Annapoorni, A. Sarkar,R. Tandon, Sens. Actuators, B, 2002, 81, 277-282.

[42] K. Hosono, I. Matsubara, N. Murayama, W. Shin,N. Izu, Thin Solid Films, 2005, 484, 396-399.

[43] J. De Souza, F. Dos Santos, B. Neto, C. Dos Santos, M. Dos Santos,C. De Melo, Sens. Actuators, B, 2003, 88, 246-259.

[44] K. Schmidt-Rohr,Q. Chen, Nat. Mater., 2007, 7, 75-83.

[45] Y. Zhang, K. Li, Q. Zhang, W. Liu, Y. Liu,C. E. Banks, New. J. Chem., 2015,

[46] K. Igarashi, M. Takiguchi,H. Ooshima, J. Ceram. Soc. Jpn., 2008, 116, 111-114.

[47] M. Takiguchi, K. Igarashi, M. Azuma,H. Ooshima, Cryst. Growth Des., 2006, 6, 1611-1614.

[48] G. C. Maiti,F. Freund, J. Chem. Soc., Dalton Trans., 1981, 949-955.

[49] K. Yamashita, K. Kitagaki,T. Umegaki, J. Am. Ceram. Soc., 1995, 78, 1191-1197.

[50] S. Nakamura, H. Takeda,K. Yamashita, J. Appl.Phys., 2001, 89, 5386-5392.

[51] A. Laghzizil, N. El Herch, A. Bouhaouss, G. Lorente,J. Macquete, J. Solid State Chem., 2001, 156, 57-60.

[52] J. Gittings, C. R. Bowen, A. C. Dent, I. G. Turner, F. R. Baxter,J. B. Chaudhuri, Acta Biomater, 2009, 5, 743-754.

[53] D. Patil, L. Patil,P. Patil, Sens. Actuators, B, 2007, 126, 368-374.